LABORATORY MODELING OF THE IONIZATION OF GAS IN A VISCOUS SHOCK LAYER

V. A. Gorelov, A. S. Korolev,
and V. S. Nikol'skii

UDC 533.6.011

The viscous shock layer (VSL) which forms due to flow around a blunt body is described by Reynolds numbers $Re_s = \rho_\infty u_\infty R/\mu_s \leq 10^3$. Here, R is the blunt radius of the body, μ_s is the viscosity of the gas behind the shock wave, and ρ_∞, u_∞ are the density of the unperturbed gas and the flow rate (the rate of flow around the blunt body under laboratory conditions). For supersonic flows the excitation processes for the internal degrees of freedom of the molecules and the processes of dissociation and ionization in the viscous shock layer are not in equilibrium. There are many studies which make numerical calculations of the thermodynamic state of the gas and the densities of its individual components (including the densities of the electrons and the ions n_e, n_i) (e.g., see the bibliography in [1]). Calculations have been made under different aircraft flight conditions using a variety of models, boundary conditions, flow rates, and calculation techniques.

The complexity of reproducing this phenomenon under laboratory conditions makes an experimental investigation of gas in a VSL difficult. There have been a few measurements of n_e in flight experiments [2, 3] and in a supersonic shock wave tunnel [4].

Under such circumstances it would be useful to generalize existing data on the ionization of gas in a VSL, to establish the corresponding correlation dependence, and to find a way of modeling this phenomenon under laboratory conditions. For this purpose calculations were made for the ionization of air in a VSL near the critical point using various gas dynamic parameters and experiments were conducted in a supersonic pulse-driven wind tunnel.

1. For determining the agreement between the results obtained from different investigations of ionization processes in a VSL, one must specify the corresponding correlation parameter. We will consider a simplified model for the ionization of air in a thin VSL near the critical point of a blunt body ($\delta \ll R$, δ is the thickness of the shock layer, and R is the blunt radius). We will assume that all the electrons which are created in the VSL because of associative ionization diffuse to a catalytic wall and recombine. We will also assume that the ionization rate corresponds to the ionization rate for air behind a shock wave. It follows from [5] that the electron density distribution behind the shock wave takes the form

$$n_e(y) = n_{ee}\varphi(\Lambda_i),$$

where n_{ee} is the equilibrium value for the electron density behind the shock wave, y is the coordinate across the shock layer, $\varphi(\Lambda_i)$ is calculated in [5] as a function of the parameter $\Lambda_i \cong R/u_\infty\tau_i$, and τ_i is the ionization time behind the shock wave (e.g., see [5, 6]).

The flow of the electron component is described by the relation

$$n_{ee}\varphi(\Lambda_i)u_\infty\varepsilon \simeq D_b\partial n_e/\partial y \sim D_b n_e/\delta, \tag{1.1}$$

where D_b is the bipolar diffusion coefficient, and $\varepsilon = \rho_\infty/\rho_s$; ρ_s is the density behind the shock wave. From (1.1) we have

$$n_e/n_{ee} \sim \mathrm{Re}_s\varphi(\Lambda_i)\varepsilon^2. \tag{1.2}$$

We will simplify expression (1.2). Direct inspection can show that for $\Lambda_i \geq 0.1$ the function $\varphi(\Lambda_i)$ is described by the dependence $\varphi(\Lambda_i) \sim \Lambda_i^2/(\Lambda_i^2 + 1)$ with acceptable accuracy. Finally, together with (1.2) we obtain for $\varepsilon \cong$ const

$$n_e/n_{ee} \sim \mathrm{Re}_s\Lambda_i^2/(\Lambda_i^2 + 1).$$

Zhukovskii. Translated from Zhurnal Prikladnoi Mekhaniki i Tekhnicheskoi Fiziki, No. 6, pp. 121-127, November-December, 1985. Original article submitted July 30, 1984.

0021-8944/85/2606-0867$09.50

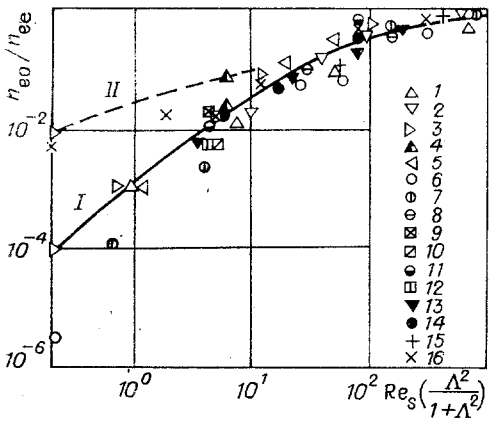

Fig. 1

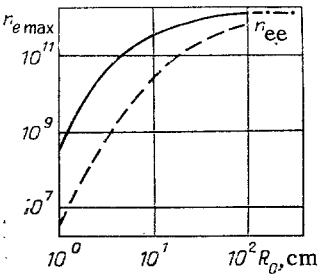

Fig. 2

However, this relation cannot be used to specify the real dependence of n_e/n_{ee} in the VSL on Re_s and Λ_i for a large range of values of the parameter $K = Re_s\Lambda_i^2/(\Lambda_i^2 + 1)$. The basic purpose of the above formulations is to isolate the correlation parameter K. The degree of correspondence between various results of determining n_e in the VSL for the dependence $n_e/n_{ee} = f(K)$ can serve as the criteria for the applicability of the parameter.

The correlation parameter K was used to process various calculation results for n_e in the VSL near the critical point and measurements for n_e made in aircraft and laboratory experiments. The results of this processing are given in Fig. 1. The quantity n_{ee}, which corresponds to the conditions of the calculations or the experiments, is determined according to [7], the value of n_e is specified near the maximum for calculations of the VSL near an object with a catalytic surface, and the quantity Λ_i, using τ_i, is taken from [5, 6]. All the results represented in Fig. 1 correspond to the case when, for making calculations of Re_s, the viscosity μ_s is found from the approximation formula in [8] for any "ideal gas".

The table defines more precisely the symbols in Fig. 1 and gives values of the gas dynamic parameters which were obtained from calculations and experiments. One notices several peculiarities in the results. In [9] calculations of n_e were made in the approximation of a thin VSL, where conditions of shock slip were neglected, and it was assumed that the vibrational degree of freedom is in thermodynamic equilibrium with the translational and rotational degrees of freedom. In [10] an analogous model for air was considered, but slip was taken into account. It was shown that slip leads to higher values of n_e. Good agreement was observed between the results of the aircraft and numerical experiments for nonequilibrium vibrational excitation in the VSL and for slip conditions [2]. In [11, 12] nonequilibrium flow in the vicinity of the critical point was considered using the complete Navier–Stokes equations.

This study conducted additional calculations of n_e using the thin VSL model for numerous values of u_∞, R, H (or ρ_∞) taking into account the dissipative processes of viscosity, thermal conductivity, and diffusion. Vibrational relaxation of the molecules O_2, N_2, and NO was considered. The transfer properties of the gas mixture are the same as those in [14]. The modified Rankin–Hugoinot conditions were imposed on the shock wave (taking into account slip). Calculations were made using a finite-difference method [15]. Both catalytic and noncatalytic surfaces with the temperature $T_w = 10^3$ were considered.

For example, Fig. 2 gives the results of calculating n_e for equilibrium (the dashed curve) and nonequilibrium (the solid curve) vibrations ($u_\infty \cong 4$ km/sec, H = 55 km, R = 1-100 cm) with a catalytic wall. It is evident from Fig. 1 that the results for a majority of the calculations and experiments, obtained for numerous gas dynamic parameters using a catalytic wall, agree well when processed with the parameter K. The results of making calculations without taking into account slip are located significantly below the average "correlation curve" I, but for $K < 50$ one can begin to observe the effects of nonequilibrium vibrations and the catalytic properties of the surface (for the latter case, see curve II for a completely noncatalytic wall).

It was established in [16] that for $u_\infty = 7$-8 km/sec the electron density in the VSL obey the law of dual similarity when $\rho_\infty R = \text{const}$ and $u_\infty = \text{const}$. This also follows from the correlation dependence in Fig. 1, since this law is satisfied for the parameter K, and $n_{ee} \sim \rho_\infty$ when $u_\infty = 6$-8 km/sec for a fair amount of accuracy.

TABLE 1

Number of point on Fig. 1	Source	H, km	v_∞, km/sec	R, cm
1	This study	55	4,0	1—10
2	»	75	7,0	1—100
3	»	85	7,8	1—100
4	»	85—100	7,3	70
5	»	55—70	6,4—7,3	1
6	[9]	45—76	6,1	2,5
7	Equilibrium vibration [2]	61—82	5,3	16
8	Nonequilibrium vibration [2]	61—82	5,3	16
9	[11]	69, 73	7,0; 7,9	1,7; 3
10	[13]	73	7,9	3
11	[12]	64,5; 73	7,9	3
12	[10]	69	7,0	3
13	Experiment [3]	70—85	7,53	15,2
14	Experiment [2]	60—80	5,3	16
15	Experiment in a shock tunnel [4]			
16	Experiment in this study			

2. Modeling of ionization processes for supersonic flow around an object requires that the laws of similarity be satisfied by the kinetic processes which occur in the gas flow. Gas dynamic modeling of equilibrium flows, as is known, assumes that the basic similarity criteria for the real and laboratory conditions are equal, which can be accomplished using supersonic wind tunnels. Modeling of the kinetic processes in the flow field of a real gas is, strictly speaking, not possible under laboratory conditions, since one must accurately reproduce the flight velocity, the real space–time scale, and the composition and thermodynamic state of the gas flow. However, it is necessary to make approximations in modeling.

The degree of nonequilibrium in the ionization processes is characterized by the relaxation parameter $\Lambda = t/\tau$, where t is the characteristic time of movement for a particle in the gas flow field, and τ is the time for ionization relaxation. For $\Lambda \gg 1$ the flow is in equilibrium, but for $\Lambda \ll 1$ the flow is "frozen" in relation to the ionization processes. Intermediate values of Λ correspond to nonequilibrium.

In sections of the flow where recombination processes prevail, $\Lambda \equiv \Lambda_r \simeq l/(u_\infty \tau_r)$ (l is the characteristic dimension of the recombination zone near the aircraft or the model, and τ_r is the characteristic recombination time). As a rule, $\tau_r \gg \tau_i$. Therefore, if the values of n_e and T are accurately reproduced in the stagnation zones near the model, then it is not possible to reproduce values of $\Lambda_r \geq 1$ in the expanding (recombination) zones of the flow, and the flow can only be modeled by "frozen" recombination.

The effects which the thermodynamic state and composition of the gas have on the ionization processes are determined by comparing the calculated and measured values of n_e at the critical point of the model. However, it is difficult to make calculations of n_e when the nonequilibrium flow possesses a complicated chemical composition.

The problem is simplified by using the correlation dependence $n_e/n_{ee} = f(K)$. One can assume that when the experimental dependence $n_e = f(R)$ at the critical point corresponds to the correlation dependence in Fig. 1 the conditions of gas dynamic modeling are fulfilled for the ionization processes in the VSL. Therefore, one can consider approximation modeling of the ionization near the aircraft using "frozen" recombination.

3. Experimental research was conducted using a pulse-driven wind tunnel (PDWT) [17]. Using such a wind tunnel allows one to obtain supersonic gas flow with high stagnation temperatures and pressures. A mixture of nitrogen and air was used as the working gas with the partial pressure ratio 10:1. Application of such a mixture makes it possible to approximate the ionization processes which occur in air [6]. The maximum values of the stagnation pressure and temperature were $p_0 = 3 \cdot 10^7$ Pa, $T_0 = 7700$ K. Obtaining such values in a PDWT posed no problems, but maintaining these values for prolonged periods of time was not possible because of intense radiative and convective heat exchange between the gas and the cold walls of the discharge chamber (Fig. 3). Measurements of the ionization levels were

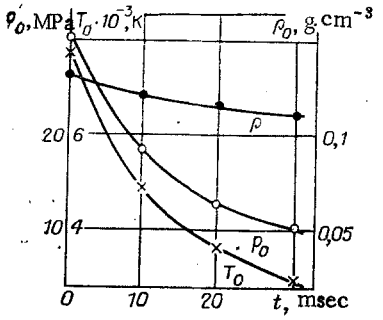

Fig. 3

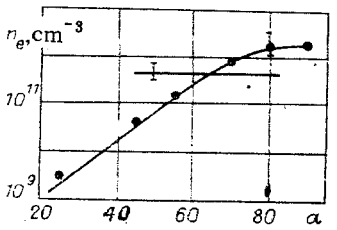

Fig. 5

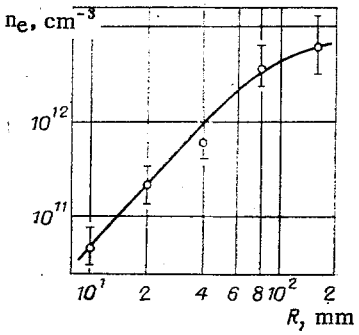

Fig. 4

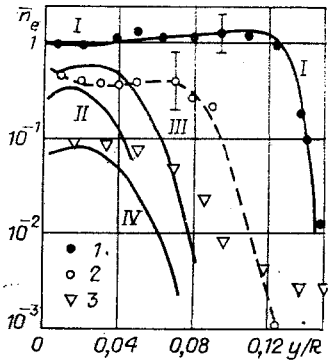

Fig. 6

made during the first 5-10 msec, when the values of p_0 and T_0 were sufficiently high.

A conical nozzle with a half-angle of $\theta = 5°$ and an output cross-sectional area of $\bar{S} = 3.07 \cdot 10^4$ was used for creating supersonic flow. For the gas parameters in the input of the nozzle which are indicated above the gas flow differs significantly from the equilibrium state. Calculations show that fluctuations in the nitrogen are "frozen" in the front section of the nozzle at a temperature of $T_v = (3\text{-}3.5) \cdot 10^3$ K, which relates to ∿7% of the total energy of the gas. The "frozen" degree of dissociation was ∿3%. The combined energy of the vibrations and the dissociation has a substantial effect on the flow parameters. The values of the statistical temperature, and, therefore, the Mach number M_∞, differ the most from their equilibrium values. For the considered PDWT mode, $M_\infty = 21$. For comparison we will show that M_∞, which is determined assuming equilibrium flow, is equal to 15-16.

Nonequilibrium flow in the nozzle leads to the presence of free electrons. Hence, the measured value of $n_{e\infty} = 10^8$ cm^{-3} agrees with the calculated value. For an equilibrium electron density of $n_{e0} = 10^{13}$ cm^{-3} at the critical point of the model (see below) with predominantly associative ionization it can be assumed that the free electrons in the flow do not have a significant effect on the ionization processes in shock layer.

For measuring n_e near the surface of the model individual cylindrical probes were used with the diameters $d_p = 0.1\text{-}0.5$ mm, and the lengths $\ell_p = 5$ mm. The probes were attached to the model with thin, insulated holders. A constant current was fed to the probes using typical methods. The feed voltage was $V_p = +4\text{-}15$ V. The probe signal was passed on to the input of a differential amplifier so that it could be registered on photorecorders.

The probe measurements were processed using the experimental results from studies of the operating features of probes in a plasma flow [18]. A simplified theory for a probe in the transfer state was applied for measuring $n_{i,e}$ near the critical point [19]. The values of $n_{i,e}$ were determined through successive approximations. The Beaumé formula for a noncollisional probe state was used as the first approximation. Successive approximations of the dimensionless flow density have the form

$$j = j_\infty j_0/(j_\infty + j_0),$$

where j_∞ and j_0 are the dimensionless flow densities for the free and collisional states [19]. Hence, the mean free path of the ions and the electrons can be calculated. It is

assumed that $T_i = T_e$. The results of noncollisional probe theory are applied for measuring n_i in the supersonic flow zones.

4. We will consider the results of measuring the electron density of the shock layer near the critical point of a blunt body for different Reynolds numbers. The measurements were made in a PDWT with $M_\infty = 21$, $u_\infty = 4.5$ km/sec, $\rho_\infty = 1.5 \cdot 10^{-7}$ g/cm^3. Different Reynolds numbers were selected by changing the spherical blunt radius R = 1-15 cm ($Re_\infty = (1.5\text{-}23) \cdot 10^3$). The obtained results are represented in Fig. 4, where the experimental points are averaged over five trials. For representing these experimental results on the correlation dependence of Fig. 1 corresponding values of Re_s, Λ_i and K were calculated. When calculating Λ_i, the ionization time τ_i in the gas mixture is found from the data in [6]. It is evident that these results correspond well with the correlation curve I for $K \geq 10$. For smaller values of K the experimental results agree better with the correlation dependence for a noncatalytic, insulated wall, which is what one would expect since the spherical blunt body is made of carbon-based glass.

Nonequilibrium ionization of the gas in a VSL for small Re leads to the appearance of interesting effects in the shock layer near an object streamlined at the angle of attack; in particular, the electron density in the shock layer on the exposed side can exceed the value of n_e near the critical point. The experimental dependence of the quantity n_e as a function of the angle of attack is shown in Fig. 5 for several points on the exposed side of an object with a form similar to a blunt, elliptical cone; the horizontal line denotes the level of the electron density near the critical point for $\alpha = 50°$, the curve represents the value of n_e, the curve represents the values of x/L = 0.8 (L is the length of the model, $Re_L = 2.7 \cdot 10^4$). It is evident that for $\alpha > 60°$ values of n_e near x/L = 0.8 exceed the value of n_e at the critical point.

The thickness of the shock layer on the exposed side of such an object increases along the chord and can substantially exceed the thickness of the VSL at the critical point. With nonequilibrium ionization this situation can lead to an increase in the electron density in the shock layer along the chord for large angles of attack to values which exceed n_e near the critical point. This effect is expressed even more distinctly for smaller values of Re.

The relative electron density distribution $\bar{n}_e = n_e/n_{ee}$ across the shock layer near the critical point is shown in Fig. 6: 1 – experimentally measured values of n_e in a nonviscous shock layer near a spherical model (R = 5 cm) in a PDWT ($M_\infty = 14$, $\rho_\infty = 4 \cdot 10^{-6}$ g/cm^3, $Re_\infty \simeq 5 \cdot 10^5$), curve I – the calculation of n_e in the layer under experimental conditions, and point 2 – the experimental results in the PDWT for $R = 8$ cm, $M_\infty = 21$, $\rho_\infty = 1.5 \cdot 10^{-7}$ g/cm^3, $Re_\infty = 1.2 \cdot 10^4$ and $K \cong 100$. The built-up front of n_e is shown conventionally. Curve II is the calculation of n_e using the theory of a thin VSL, and curve III shows the results obtained using [12] (calculations with the Navier–Stokes equations) for similar values of the parameter K. The numeral 3 denotes the experimental results of [4] obtained in a supersonic shock tunnel with $M_\infty = 13$, $\rho_\infty = 1.8 \cdot 10^{-7}$ g/cm^3, $u_\infty = 4.5$ km/sec, $Re_\infty = 3.2 \cdot 10^3$, $K \simeq 60$. Curve IV represents calculations using the theory of a thin VSL without taking into account the electron density in the incident flow, whose level in this case is sufficiently high ($n_{e\infty} = 10^{10}$cm^{-3}). These data allow one to find a way to measure the profile of the electron density across the shock layer for decreasing Re and for a transition to the VSL state.

One should note that when the maximum values of n_e obtained through calculations and experiments agree well, the experimentally measured profile of $\bar{n}_e$ is "filled out" more. Better correspondence between the distribution $\bar{n}_e$ from [4] and that from calculations was obtained in [13], where the values of $n_{e\infty}$ in the incident flow were taken into account. However, for the results obtained in the PDWT for K = 100 it is not necessary to take into account $n_{e\infty}$ because it is fairly small.

The discrepancies between the calculated and experimental profiles for $\bar{n}_e$ evidently require additional theoretical and experimental investigations into the nonequilibrium ionization processes in a viscous shock layer.

The authors express their gratitude to M. K. Gladyshev for his help in conducting the experiments.

LITERATURE CITED

1. "Nonequilibrium ionization during the motion of supersonic aircraft," Summary from the Department of Scientific and Technical Information (ONTI) at the N. Ye. Zhukovskii Central Institute of Aerohydrodynamcs (TsAGI), No. 527 (1977).

2. D. T. Hayes, "Electrostatic probe measurements of flow field characteristics of a blunt body reentry vehicle," AIAA Paper, No. 72, 694 (1972).
3. P. W. Huber, J. S. Evans, and C. J. Schexnayder, "Comparison of theoretical and flight-measured ionization in a blunt body reentry flow field," AIAA Paper, No. 70, 756 (1970).
4. E. M. Kaegi and D. L. McMenamin, "Measured and predicted air ionization in blunt body shock layers," AIAA Paper, No. 69, 81 (1969).
5. O. Yu. Polyanskii and G. N. Sayapin, "Nonequilibrium electron density behind a shock wave near a blunt body in a supersonic flow of air," Scientific notes, N. Ye. Zhukovskii Central Institute of Aerohydrodynamics (TsAGI), 9, No. 4 (1978).
6. J. H. Schafer and A. Frohn, "Ionization behind shock waves in nitrogen–oxygen mixtures," AIAA J., 10, No. 8 (1972).
7. J. Martin, Entry into the Atmosphere [Russian translation], Mir, Moscow (1969).
8. V. N. Gusev and V. P. Provotorov, "Modeling supersonic flows of ionized gas in wind tunnels," Transactions from the N. Ye. Zhukovskii Central Institute of Aerohydrodynamics (TsAGI), No. 2111 (1981).
9. F. G. Blottner, "Viscous shock layer at the stagnation point with nonequilibrium air chemistry," AIAA J., 7, No. 12 (1969).
10. J. C. Adams, "Shock slip analysis of merged layer stagnation point air ionization," AIAA J., 8, No. 5 (1970).
11. A. Kumar and A. C. Jain, "Nonequilibrium merged stagnation shock layers at hypersonic speeds," Int. J. Heat Mass Transfer, 18, No. 10 (1975).
12. G. F. Withoff and K. J. Victoria, "On a solution of the unsteady Navier–Stokes equations including multicomponent finite rate chemistry," Comput. Fluids, 1, No. 2 (1973).
13. T. C. Dellinger, "Computation of nonequilibrium merged stagnation shock layers," AIAA J., 9, No. 2 (1971).
14. V. G. Voronkin, "Nonequilibrium viscous shock layers for blunt cones," Izv. Akad. Nauk SSSR, Mekh. Zhidk. Gaza, No. 6 (1979).
15. V. S. Nikol'skii, "A technique for calculating nonequilibrium viscous flow during supersonic flow around blunt bodies," Transactions from the N. Ye. Zhukovskii Central Institute of Aerohydrodynamics (TsAGI), No. 2043 (1980).
16. V. N. Gusev, V. P. Provotorov, and V. V. Ryabov, "The role of physical and chemical processes in the modeling of low density gas flows," Scientific notes from the N. Ye. Zhukovskii Central Institute of Aerohydrodynamics (TsAGI), 12, No. 4 (1981).
17. A. S. Korolev, B. V. Boshenyatov, I. G. Druker, and V. V. Zatoloka, Pulse-Driven Wind Tunnels in Aerodynamic Studies [in Russian], Nauka, Novosibirsk (1978).
18. V. A. Gorelov, L. A. Kil'dyushova, and V. M. Chernyshev, "Measuring the ionization of air behind intense shock waves," Teplofiz. Vys. Temp., 21, No. 3 (1983).
19. P. Chan, L. Talbot, and K. Turyan, Electrical Probes in Motionless and Moving Plasma [Russian translation], Mir, Moscow (1978).